DEUTSCHES ELEKTRONEN-SYNCHROTRON DESY

DESY SR 90-04
June 1990

Reflectance and Total Photoelectric Yield Measurements of Silicon Wafers in the XUV Spectral Range.

F.-R. Bartsch, H.-G. Birken, C. Kunz, R. Wolf
II. Institut für Experimentalphysik, Universität Hamburg

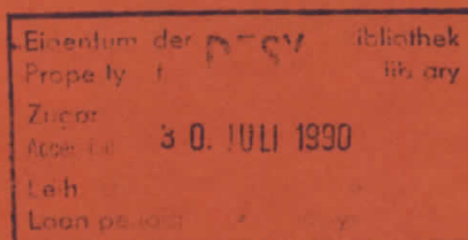

ISSN 0723-7979

NOTKESTRASSE 85 · 2 HAMBURG 52

DESY behält sich alle Rechte für den Fall der Schutzrechtserteilung und für die wirtschaftliche Verwertung der in diesem Bericht enthaltenen Informationen vor.

DESY reserves all rights for commercial use of information included in this report, especially in case of filing application for or grant of patents.

To be sure that your preprints are promptly included in the
HIGH ENERGY PHYSICS INDEX ,
send them to the following address (if possible by air mail) :

DESY
Bibliothek
Notkestrasse 85
2 Hamburg 52
Germany

Reflectance and Total Photoelectric Yield Measurements of Silicon Wafers in the XUV Spectral Range

F.-R. Bartsch, H.-G. Birken, C. Kunz, and R. Wolf
II. Institut für Experimentalphysik, Universität Hamburg,
Luruper Chaussee 149, 2000 Hamburg 50, FRG

Abstract

We present reflectance and total photoelectric yield measurements of commercially available silicon wafers. The measurements have been performed at the XUV reflectometer station at HASYLAB (DESY) between 50 and 900 eV photon energy. Fitting of the reflectance as a function of angle of incidence using Fresnel's equations yielded values for the thickness of the native oxide layer and optical constants of the Si-wafer. The surface roughness of Si-wafers could also be determined. The optical constants derived from angular dependent total photoelectric yield measurements are in good agreement with those obtained from reflectance measurements on the same Si-wafer. Some of the Si-wafers investigated were cleaned by a combination of chemical etching and in-situ thermal treatment in order to reduce the oxide layer. Si-wafers which were solely etched revealed an oxide layer clearly thinner than that of unetched samples as well as a drastic decrease of their surface roughness. Subsequent in-situ thermal treatment resulted in oxide-free Si-wafers. This treatment, however, always brought about a strong increase in surface roughness.

to be published in J. Phys.

ISSN 0723-7979

1. Introduction

The optical properties of thin layers in the XUV spectral region are important for the developement of optical devices which are applied in plasma physics, synchrotron radiation physics, and space astronomy. The structure of the SiO_2-Si-interface and its optical properties are of interest for many applications and have been the subject of many investigations [1-4]. Different preparations strongly influence the structure and thus the optical and electronic properties of thin layers. We have measured the reflectance as well as the total photoelectric yield of commercially available Si-wafers in dependence of the angle of incidence between 50 and 900 eV photon energy with the aim to investigate the optical behaviour of SiO_2-Si-interfaces prepared by different methods.

The optical properties of a material can be described by the energy dependent dielectric constant $\tilde{\varepsilon}(\hbar\omega) = \varepsilon_1 + i \cdot \varepsilon_2$, which is related to the complex index of refraction by $\tilde{\varepsilon} = \tilde{n}^2$. The reflectance of a plane bounded, semi-infinite material can be calculated with Fresnel's reflectance equations [5], which depend on the angle of incidence and the polarization of the incident radiation as well as on the dielectric constant of the reflecting material. The reflectance of a Si-wafer, which is covered with a thin SiO_2-layer, also depends on the dielectric constant and the thickness of the oxide layer, and Fresnel's equations for a film on a substrate have to be used. Due to surface roughness, which is present on all real samples, some of the incident radiation is reflected into non-specular directions. This results in a diffuse straylight distribution concentrated about the reflected beam. The influence of the surface roughness on the specular reflectance can theoretically be taken into account by multiplying a factor $exp[-(4\pi \cdot \delta_r \cdot \cos\theta/\lambda)^2]$ [6], where δ_r, θ, λ denote the rms-roughness, the angle

of incidence, and the vacuum wavelength respectively. Reflectance versus angle of incidence spectra are evaluated by least-squares-fits.

The photoelectric yield versus angle of incidence can theoretically be described in terms of the dielectric constant of the photoemissive material and an average electron escape depth. Pepper developed a rigorous formalism to calculate the angular dependent photoelectric yield for a thin film on a substrate [7]. The central assumption in this model is that the number of escaping photoelectrons is proportional to the amount of energy absorbed in the topmost layer of the sample. The photoelectron escape probability is given by a weight factor exponentially decaying with distance from the surface. The equations are valid for arbitrary values of the dielectric constants of the film and of the substrate. They are given for s- and p-polarized radiation. We have shown for Al [8], Cu and Pt [9] that the photoelectric yield measured as a function of angle of incidence contains sufficient information to obtain precise values of the optical constants and of the film thickness.

2. Experiment

The experiments have been performed at the synchrotron radiation laboratory HASYLAB. Our experimental setup consists of a plane grating monochromator and an UHV-reflectometer. The monochromator supplies the reflectometer with radiation of photon energy between 50 and 1200 eV. Its principles and characteristics have been described in reference [10]. A toroidal mirror behind the exit slit of the monochromator refocusses the beam; at the sample, the beam size is $0.85 \times 2.2\,mm^2$ (FWHM, vert. × horiz.) and its divergence is $2.1 \times 4.8\,mrad^2$. The reflectometer provides computer-controlled independent rotation and translation of sample and detector. Details of the reflectometer are given in reference [11]. The reflectance measurements were performed with a semiconductor diode (Hamamatsu G1127) in connection with a Keithley 617 electrometer. The characteristics of this diode have been reported elsewhere [12]. The aperture of the detector is $1.0 \times 2.6\,mm^2$ (vert. × horiz.); the distance between sample and detector is 150 mm. Since the sample can be removed from the direct beam, normalization of the spectra can be done by moving the detector into the direct beam and measuring the incident photon flux. Corrections for changes in the incoming photon flux are made by monitoring the total electron yield from the kanigen coated toroidal mirror in front of the reflectometer.

For the photoelectric yield measurements the sample was surrounded with an electron collector, which is designed not to interfere with the incident and reflected light beams. The potential difference between the sample and the collector was 15 V; the actual yield signal was accomplished by monitoring the photocurrent leaving the silicon sample.

The silicon samples were measured as obtained from the manufacturer or they were

submitted to an etching procedure described in reference [13] prior to loading into the vacuum system. This etching procedure, which is based on repetitive wet oxide removal and re-oxidation of the silicon wafer, is commonly employed to remove contaminants such as carbon and heavy metals. Furthermore, the oxide layer produced by this method should be thinner and more volatile than the native oxide layer of the silicon wafer, making it possible to remove this oxide layer by heating at a lower temperature than the native oxide [13]. After cleaning and final oxidation (etching) the samples were kept wet with ethanol, to prevent direct contact with the atmosphere during mounting them into the reflectometer. Before the measurements could be started a pumping period of 20 h was necessary to establish UHV conditions. The mean pressure during this time was about $P \simeq 10^{-5}$ Pa. Some of the samples were tempered by ohmic heating for about 20 min at 900°C temperature in order to completely remove the oxide layer. Although the tempering process was performed under UHV conditions the reflectometer pressure rose up to $P \simeq 10^{-4}$ Pa during heating. Immediately after tempering the pressure rapidly decreased and the base pressure of about $P \simeq 10^{-8}$ Pa could be restored within 20 min. The success of the temper process was controlled by reflectance versus photon energy spectra at the Si-$L_{2,3}$ edge and at the O-K edge taken at $\theta = 85°$ angle of incidence. The disappearance of the modulation in the reflectance spectra at the O-K edge was considered an indicator of a successful reduction of the oxide.

3. Results

The inset of Fig. 1 shows the principle of a straylight spectrum. The sample is put into the beam under a fixed angle and the detector is rotated from grazing angle through the specular reflex, until the signal vanishes into noise. A set of straylight spectra taken at differently treated samples from the same wafer is presented in Fig. 1 together with specular reflectance vs. angle of incidence measurements. For specular reflectance measurements the sample is rotated by an angle decrement $\Delta\theta$ and the detector rotates at the same time by $2\Delta\theta$, see inset Fig. 2. Both, the decrease in specular reflection and the wings in the straylight spectra provide information on surface topography, in general surface roughness.

In Fig. 1 reflectance and straylight spectra measured at $\theta_i = 80°$ angle of incidence at $\hbar\omega = 120\,eV$ photon energy ($\lambda = 10.33\,nm$ wavelength) from differently prepared samples are compared. Dotted lines indicate spectra of the unprepared wafer, dashed curves originate from the etched sample, and dash-dotted lines represent the tempered wafer. The asymmetry in the angular distribution of the staylight can be explained in terms of the optical constants and of the roughness parameters of the silicon wafers [14]. A qualitative comparison of the straylight spectra shows the etched sample to be smoothest followed by the unprepared one. Tempered wafers revealed the roughest surfaces. Differences in reflectance between etched and unprepared samples are rather small. The lower reflectance of the tempered wafer partially results from its increased roughness but mainly from the loss of the oxide layer.

For quantitative data analysis we used Fresnel's equations in a least-squares-fit

procedure. The χ^2-function

$$\chi^2 = \sum_{i=1}^{n} \frac{1}{\sigma_i^2} |R_{exp}(\theta_i) - R_{theo}(\theta_i, \bar{\varepsilon}_{SiO_2}, \bar{\varepsilon}_{Si}, d, \delta_r, P)|^2$$

was minimized, whereby $\bar{\varepsilon}_{SiO_2}$ and $\bar{\varepsilon}_{Si}$ denote the optical constants of silicon oxide and silicon. d is the thickness of the oxide layer and δ_r the rms-roughness. The polarization P of the incident radiation entered the χ^2-function as a constant parameter. σ_i represents the statistical error of each experimental point, which was estimated to be 1% of the measured $R(\theta)$-value. Figs. 2a and 2b show the measured $R(\theta)$-curve (ooo) of a naturally oxidized silicon wafer at $\hbar\omega = 120$ eV photon energy together with fitted curves (- - -). The fit of Fig. 2a is based on the assumption of a homogeneous bulk material, whereas the fit of Fig. 2b considers an oxide layer which is supported by a bulk silicon. Each point of the dotted line in the middle of Figs. 2a and 2b shows the difference between the theoretical and the experimental reflectance value in units of σ_i. A comparison of these two fits clearly favours the film model although no visual interference patterns can be discerned in the spectrum as one would expect with a thicker oxide layer. The discontinuity in the "theory minus experiment" curve near 70 degrees angle of incidence is due to a slight mismatch between different ranges of the current meter, which does not affect our data analysis.

The optical constants of the bulk silicon $\bar{\varepsilon}_{Si}$, the film thickness d, and the vacuum interface roughness δ_r served as free fit parameters. In order to avoid overinterpreting our experimental data the optical constants of the silicon oxide film $\bar{\varepsilon}_{SiO_2}$ served as fixed parameters in the fit procedure. They have been determined from angular dependent reflectance measurements of "white crown" glass performed earlier [15]. This glass consists by roughly 70 % of silicon oxide and by smaller fractions of alkali oxides with most of their absorption edges outside the spectral range covered here. In all cases completely s-polarized radiation was assumed. It has been verified earlier that the fit results do not depend on the degree of polarization as long as it is above 85 % s-polarization as is the case in our experiment [8].

From the fit procedure we obtained an oxide layer thickness of unprepared wafers of about 1.2 nm. In the case of etched wafers we found a film thickness of about 0.7 nm. Surface roughness of the natural oxide layer was determined to be about 0.5 nm, whereas etched silicon wafers showed a roughness of less than 0.1 nm. Tempering of the wafers resulted in a strong decrease of specular reflectance as well as a significant increase of diffusely scattered light (Fig. 1) which is attributable to an enhanced surface roughness. We found up to 3 nm roughness depending on the degree of misorientation of the silicon wafers. According to the manufacturer's statement the Si(111) samples we used have a smaller degree of misorientation than the Si(100) samples. This appears to cause the smaller roughness of (111)-oriented samples after tempering (1.1 nm) compared with the 3.0 nm of (100)-oriented silicon. Some results for surface roughness and film thickness of different samples are summarized in table 1. We found the increase in roughness after tempering to be independent of the way of sample preparation. Thicknesses determined at many different photon energies were in excellent agreement with each other. This is especially noteworthy in view of the large differences in absorption of Si and SiO_2 below and above the Si-$L_{2,3}$ and O-K edges. Also the roughness data are remarkably independent of the wavelenght.

The reflectance curves of unprepared and etched wafers excellently fitted to Fresnel's equations. With the tempered wafers, however, the agreement between theoretical and experimental data was somewhat lesser whereby bulk fits were of superior quality compared with those assuming a film on top. This indicates that no homoge-

neous film is left on the surface. It cannot be excluded, however, that small amounts of oxide molecules or molecules other than pure silicon are left on the surface and influence the reflectance spectra. An increase in pressure during tempering as mentioned in the experimental section may contribute to a contamination of the surface.

Fig. 3 shows the real and imaginary part of the dielectric function $\tilde{\epsilon}$ of silicon as determined by the fits of different samples represented by different symbols (tables 2, 3 and 5). Data obtained from fits are compared with the real and imaginary part of the dielectric function calculated from atomic scattering factors given by Henke et al. [16] and from data given by Edwards [17]. Agreement above the Si-$L_{2,3}$ edge is good. Differences at the Si-$L_{2,3}$ edge are due to the fact that the method of compilation used by Henke et al. gives no reliable data for the shape of the dielectric function around absorption edges [16]. Comparing our data with those published by Klingenberg et al. [3] we find good agreement. Agreement with data published by Windt et al. [4] is poor. The authors indicate that their samples might have been oxidized although the evaluation was performed under the assumption that the sample was pure silicon.

A comparison of the real and imaginary part of the dielectric function derived from reflectance measurements with data from angular dependent photoelectric yield measurements performed near the Si-$L_{2,3}$ edge shows quite good agreement (tables 3, 4). These data were obtained by fitting a simple bulk model to the spectra taken from an oxidized wafer thereby neglecting the influence of the oxide on the yield spectra. We assume that the oxide layer's contribution to the total electron emission is rather small compared with the emission from the silicon substrate. Fig. 4 shows a fit of a yield spectrum at 120 eV. The spectrum was normalized to the yield at normal incidence. Circles denote the experimental spectrum, a dashed line the theory, and points give

the difference between theory and experiment in units of the standard deviation σ_i. The fit results in data for the real and imaginary part of the dielectric function $\tilde{\epsilon}$ of silicon as well as the value of the electron escape depth. Since it is assumed in the yield model that reflected and scattered radiation sums up to the specular reflection of a smooth surface there is no parameter for surface roughness.

Fig. 5 shows the data by Henke et al. and Edwards as above. Denoted by circles the real and imaginary part of the dielectric function from yield measurements is compared with data from reflectance measurements taken at the same sample without breaking the vacuum. Agreement of these data with those from reflectance measurements is noteworthy and underlines the significance of optical constants derived from angular dependent yield spectra.

4. Summary

In conclusion, we have demonstrated that a nondestructive determination of film thickness and surface roughness can be achieved by angular dependent reflectance measurements. In addition, the optical constants of silicon in the XUV-range from 50 to 900 eV have been determined. The comparison of these optical constants with data given by other authors and with data determined by total yield measurements show good agreement.

This work was supported by the Bundesminsterium für Forschung und Technologie under contract no. 05 405AX B/5 KU.

References

[1] F.C. Brown, R.Z. Bachrach, and M. Skibowski,
Phys. Rev. B **15**, 4781 (1977)

[2] O.A. Ershov and A.P. Lukirskii,
Soviet Physics Solid State **8(7)**, 1699 (1967)

[3] E.-D. Klingenberg, W. Blau, P.P. Illinsky, and E.S. Gluskin,
Nucl. Instr. Meth. A **261**, 140 (1987)

[4] D.L. Windt, W.C. Cash, M. Scott, P.Arendt, B. Newman,
R.F.Fisher, A.B. Swartzlander, P.Z. Takacs, and J.M. Pinneo,
Appl. Opt. **27(2)**, 279 (1988)

[5] M. Born and E. Wolf,
"Principles of Optics," 5th Ed.,Pergamon Press Ltd., Oxford 1975

[6] P. Beckmann and A. Spizzichino,
"The Scattering of electromagnetic Waves from rough Surfaces,"
Pergamon Press Int, New York 1963

[7] S.V. Pepper,
J. Opt. Soc. Am. **60**, 805 (1970)

[8] H.G. Birken, W. Jark, C. Kunz, and R. Wolf,
Nucl. Instr. Meth. A **253**, 166 (1986)

H.G. Birken, C. Blessing, and C. Kunz,
Determination of Optical Constants from Angular-Dependent
Photoelectric-Yield Measurements, in E.D. Palik ed.,
"Handbook of Optical Constants of Solids Vol.2,"
(Academic Press, Orlando 1990) to be published

[9] H.G. Birken, C. Blessing, C. Kunz, and R. Wolf,
Rev. Sci. Instrum. **60**, 2223 (1989)

[10] W. Jark and C. Kunz,
Nucl. Instr. and Meth. A **246**, 320 (1986)

[11] H. Hogrefe, D. Giesenberg, R.P. Haelbich, and C. Kunz,
Nucl. Instr. and Meth. **208**, 415 (1983)

[12] M. Krumrey, J. Barth, E. Tegeler, M. Krisch, F. Schäfers, and R. Wolf,
Appl. Opt. **27**, 4336 (1988)

[13] A. Istizaka, K. Nakagawa, and Y. Shiraki,
Coll. Pap. of MBE-CST-2, 183, Tokyo 1982

[14] H.-G. Birken, C. Kunz, and R. Wolf,
Physica Scripta Vol.41, p.385 1989

[15] C. Blessing, Diploma-Thesis, Hamburg 1988,
Internal Report, HASYLAB 88-11, 1988

[16] B.L. Henke, P. Lee, T.J. Tanaka, R.L. Shimambukuro, and B.K. Fujikawa,
Atomic Data and Nuclear Data Tables **27**,1(1982)

[17] D.F. Edwards, Silicon, in E.D. Palik ed.,
"Handbook of Optical Constants of Solids,"
Academic Press, Orlando 1985, p. 547

Table 1: Oxide layer thickness and surface roughness on silicon

Sample	119.9 eV Film thickness [nm]	119.9 eV Roughness [nm]	522.2 eV Film thickness [nm]	522.2 eV Roughness [nm]
Si(100), unprep.	1.16 ± 0.04	0.37 ± 0.01	1.17 ± 0.19	0.65 ± 0.08
Si(111), unprep.	1.08 ± 0.02	0.40 ± 0.01	1.25 ± 0.07	0.30 ± 0.07
Si(100), etched	0.80 ± 0.04	0.15 ± 0.04	0.77 ± 0.01	$< 0.1 \pm 0.07$
Si(111), etched	0.96 ± 0.02		$< 0.1 \pm 0.04$	
Si(100), tempered		2.84 ± 0.01		2.20 ± 0.01
Si(111), tempered		1.34 ± 0.01		1.08 ± 0.01

Table 2: Silicon(100), unprepared; R(θ)-measurements

$\hbar\omega/eV$	$1-\epsilon_1$	ϵ_2	$1-N$	κ
47.6	9.610E-02	1.442E-02	4.923E-02	7.581E-03
71.8	3.182E-02	6.990E-03	1.603E-02	3.552E-03
95.4	-5.836E-03	2.815E-03	-2.915E-03	1.403E-03
100.5	-4.229E-02	1.933E-02	-2.097E-02	9.464E-03
105.6	-2.101E-02	2.223E-02	-1.051E-02	1.100E-02
109.9	-2.167E-02	2.954E-02	-1.088E-02	1.461E-02
119.9	-8.483E-03	4.393E-02	-4.471E-03	2.187E-02
503.5	3.584E-03	9.380E-04	1.793E-03	4.699E-04
522.2	3.370E-03	7.996E-04	1.687E-03	4.005E-04
540.7	3.155E-03	7.257E-04	1.579E-03	3.634E-04
550.3	3.002E-03	7.095E-04	1.502E-03	3.553E-04

Table 3: Silicon(111), unprepared; R(θ)-measurements

$\hbar\omega/eV$	$1-\epsilon_1$	ϵ_2	$1-N$	κ
95.3	-9.241E-03	8.505E-04	-4.610E-03	4.233E-04
100.0	-2.144E-02	3.274E-02	-1.080E-02	1.620E-02
103.7	-1.174E-02	2.006E-02	-5.900E-03	9.971E-03
119.9	-6.532E-03	4.120E-02	-3.471E-03	2.053E-02
190.6	1.452E-02	1.720E-02	7.247E-03	8.662E-03
522.1	3.269E-03	7.822E-04	1.636E-03	3.917E-04
540.7	3.040E-03	7.135E-04	1.521E-03	3.573E-04
763.8	1.477E-03	1.958E-04	7.389E-04	9.798E-05
864.4	1.171E-03	1.477E-04	5.858E-04	7.387E-05

Table 4: Silicon(111), unprepared; G(θ)-measurements

$\hbar\omega/eV$	$1-\epsilon_1$	ϵ_2	$1-N$	κ
95.3	-5.570E-03	6.729E-03	-2.787E-03	3.355E-03
98.4	-3.003E-02	1.889E-03	-1.491E-02	9.306E-04
100.4	-2.611E-02	4.139E-02	-1.318E-02	2.043E-02
102.8	-2.157E-02	2.696E-02	-1.082E-02	1.333E-02
107.4	-2.294E-02	3.871E-02	-1.159E-02	1.913E-02
109.9	-3.309E-02	3.640E-02	-1.657E-02	1.790E-02
119.9	-3.767E-03	4.383E-02	-2.120E-03	2.187E-02
192.5	1.519E-02	1.969E-02	7.573E-03	9.922E-03
522.2	3.004E-03	7.483E-04	1.503E-03	3.747E-04
531.4	2.986E-03	1.018E-03	1.494E-03	5.099E-04
540.7	2.848E-03	8.740E-04	1.425E-03	4.376E-04

Table 5: Silicon(100), etched; R(θ)-measurements

$\hbar\omega/eV$	$1-\epsilon_1$	ϵ_2	$1-N$	κ
95.3	-5.669E-03	3.051E-03	-2.832E-03	1.521E-03
100.0	-4.509E-02	9.904E-03	-2.231E-02	4.844E-03
109.9	-3.443E-02	1.970E-02	-1.712E-02	9.683E-03
119.9	-1.368E-02	3.582E-02	-6.975E-03	1.778E-02
144.2	6.638E-03	3.025E-02	3.209E-03	1.517E-02
190.6	1.655E-02	1.884E-02	8.264E-03	9.498E-03
192.5	1.399E-02	1.649E-02	6.986E-03	8.304E-03
238.2	1.270E-02	9.872E-03	6.359E-03	4.967E-03
285.8	9.405E-03	6.488E-03	4.708E-03	3.259E-03
334.2	7.516E-03	3.605E-03	3.764E-03	1.809E-03
377.8	6.049E-03	2.457E-03	3.028E-03	1.232E-03
426.0	4.831E-03	1.629E-03	2.418E-03	8.167E-04
474.9	3.885E-03	1.143E-03	1.944E-03	5.726E-04
522.1	3.300E-03	8.882E-04	1.651E-03	4.448E-04
535.1	3.057E-03	7.898E-04	1.530E-03	3.955E-04
540.7	3.037E-03	7.384E-04	1.520E-03	3.697E-04
569.7	2.717E-03	6.259E-04	1.360E-03	3.134E-04
619.6	2.284E-03	4.736E-04	1.143E-03	2.371E-04
714.7	1.711E-03	2.809E-04	8.556E-04	1.406E-04
763.8	1.496E-03	2.509E-04	7.482E-04	1.256E-04
814.7	1.314E-03	1.935E-04	6.574E-04	9.681E-05
864.4	1.170E-03	1.895E-04	5.854E-04	9.483E-05

Figure captions

Fig 1: Reflectance R(θ) vs. angle of incidence θ and straylight at fixed angle of incidence $\theta_0 = 80^\circ$ for different scattering angles θ of differently treated silicon wafers at $\hbar\omega = 120\,eV$. Dotted lines: unprepared wafer; dashed lines: etched wafer; dash - dotted lines: tempered wafer. Inset: principle of straylight spectra.

Fig 2a: Reflectance R(θ) vs. angle of incidence θ at $\hbar\omega = 120\,eV$. Circles: measured reflectance of unprepared wafer; dashes: fit to experimental curve with bulk model; dots: deviation of theory minus experiment in units of σ_i. Inset: principle of reflectance spectra.

Fig 2b: Reflectance R(θ) vs. angle of incidence θ at $\hbar\omega = 120\,eV$. Circles: same reflectance spectrum as Fig. 2a; dashes: fit to experimental curve with film model; dots: deviation of theory minus experiment in units of σ_i.

Fig 3: Real part $1 - \epsilon_1$ and imaginary part ϵ_2 of the dielectric function $\tilde{\epsilon}$ of silicon vs. photon energy $\hbar\omega$. Circles, squares and diamonds represent fit results of different samples; dotted line: data from Edwards [17]; continuous line: calculated from atomic scattering factors from Henke et al. [16].

Fig 4: Total photoelectric yield G(θ) vs. angle of incidence at $\hbar\omega = 120\,eV$. Circles: experimental curve; dashes: theory; dots: deviation of theory minus experiment in units of σ_i.

Fig 5: Comparison of fit results from reflectance and from yield spectra of the same sample. Circles: yield; squares: reflectance; dotted line: dielectric function from data given by Edwards [17]; continuous line: dielectric function calculated from atomic scattering factors by Henke et al. [16].

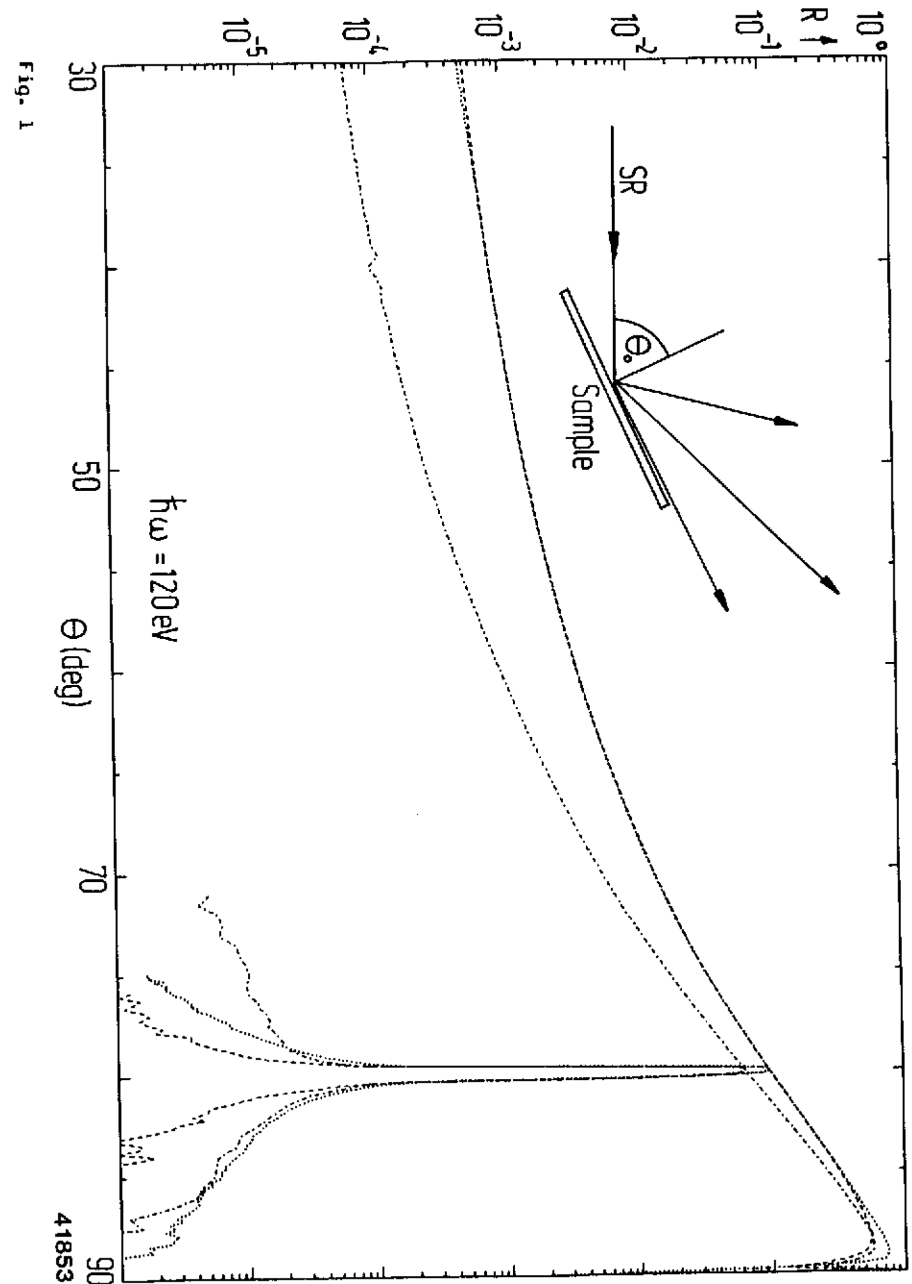

Fig. 1

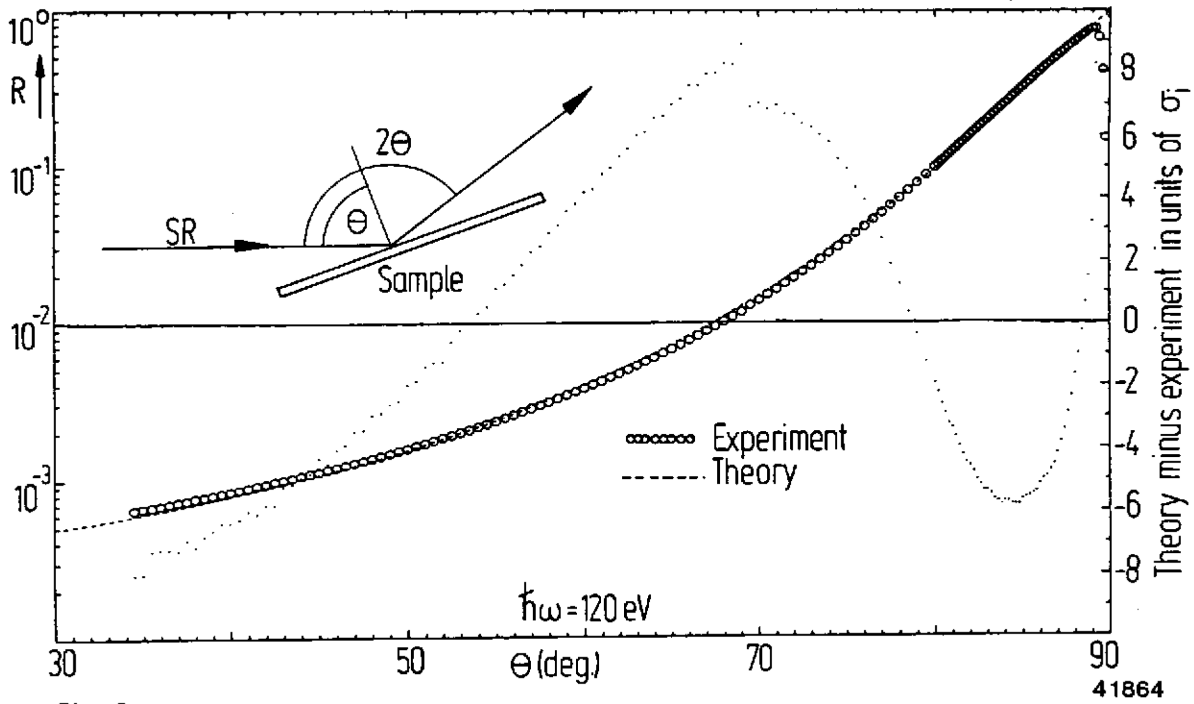

Fig. 2a

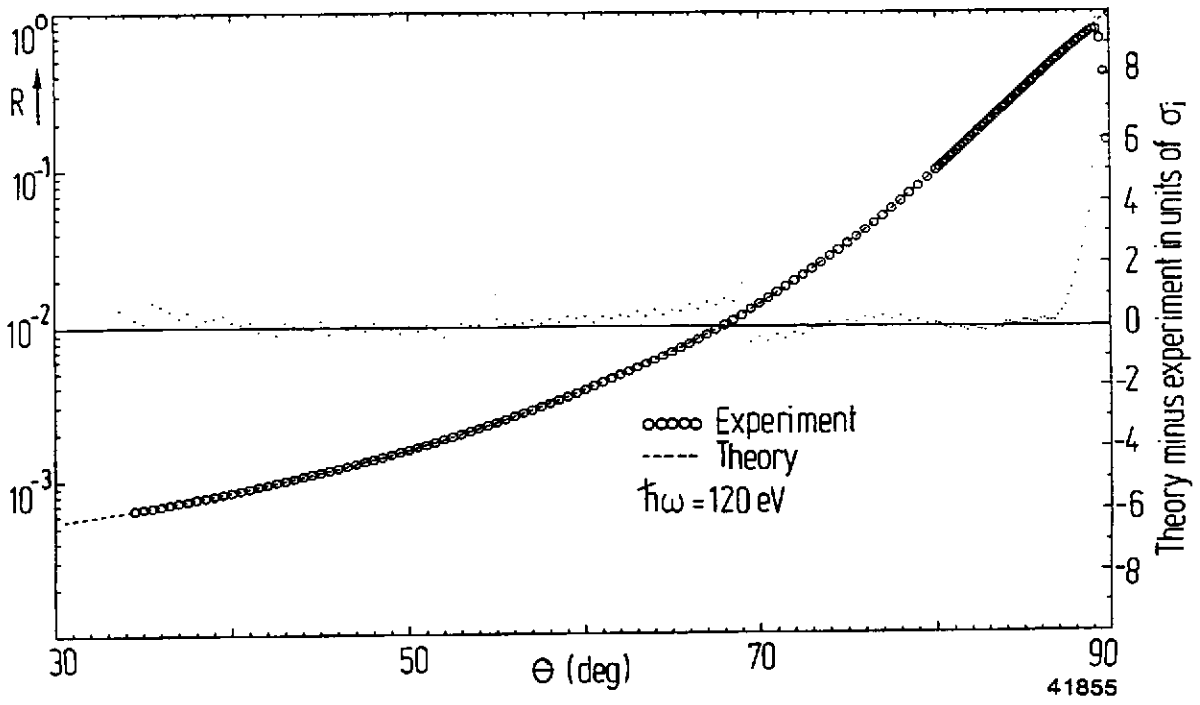

Fig. 2b

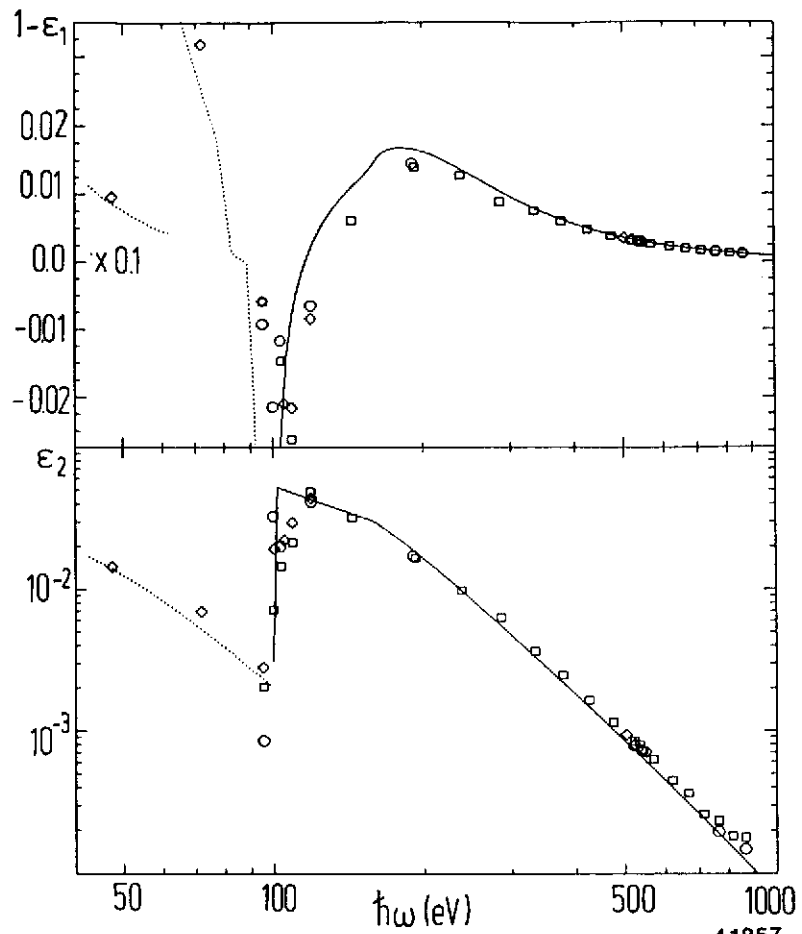

Fig. 3

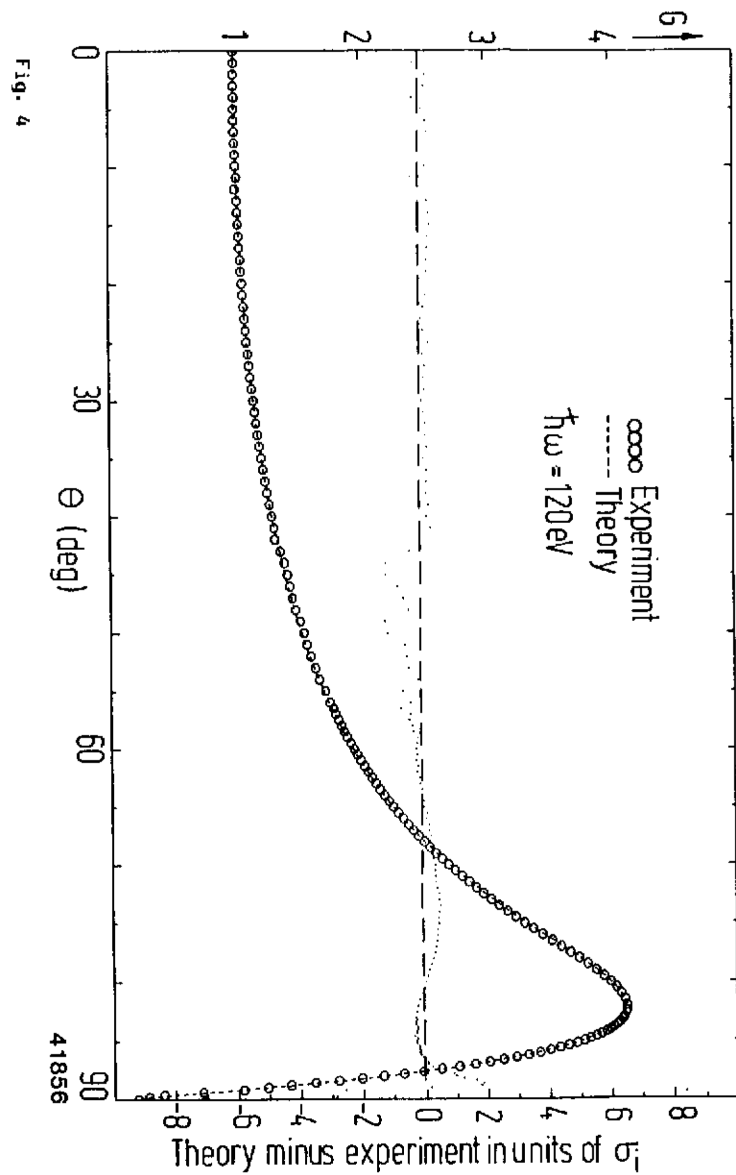

Fig. 4

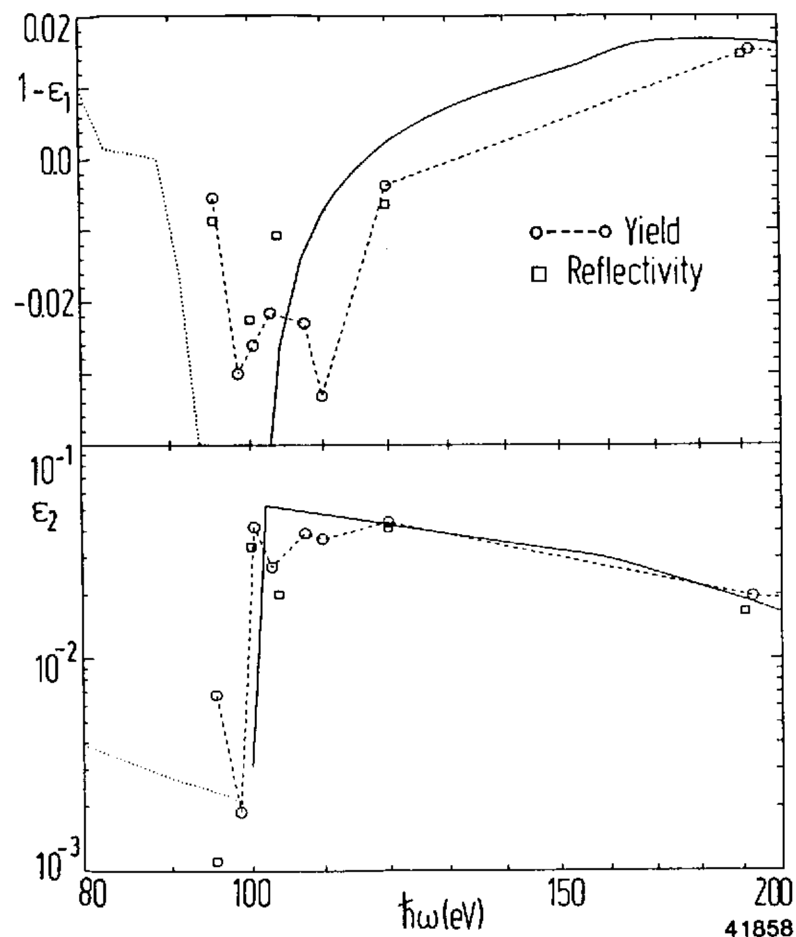

Fig. 5